Available online at www.sciencedirect.com

ScienceDirect

Journal of the European Ceramic Society 28 (2008) 2947–2953

www.elsevier.com/locate/jeurceramsoc

Synthesis and performances of Ni–SDC cermets for IT-SOFC anode

Min Chen[a], Bok Hee Kim[a,*], Qing Xu[b,**], O. Jeong Nam[a], Jung Hoon Ko[a]

[a] *Department of Hydrogen and Fuel cells Engineering, Hydrogen & Fuel Cell Research Center,*
Chonbuk National University, Jeonju, Jeonbuk, 561-756, South Korea
[b] *School of Materials Science and Engineering, Wuhan University of Technology, Wuhan, 430070, PR China*

Received 6 April 2008; accepted 13 May 2008
Available online 24 June 2008

Abstract

NiO–SDC (samaria-doped ceria) composite powders were synthesized using a urea-combustion technique. The structure, electrical conducting, thermal expansion and mechanical properties of the Ni–samaria-doped ceria (Ni–SDC) cermets have been investigated with respect to the volume contents of Ni. No chemical reaction product between the two constituents was detected for the cermets sintered at 1200–1300 °C for 4 h in air and reduced at 800 °C for 2 h in a $60\%N_2 + 40\%H_2$ atmosphere. A porous microstructure consisting of homogeneously distributed Ni and SDC phases together with well-connected grains was observed. It was found that the open porosity, electrical conductivity, thermal expansion and bending strength of the cermets are sensitive to the volume content of Ni. The Ni–SDC cermets containing 50–60 vol.% Ni were ascertained to be the optimum composition. These compositions offer sufficient open porosity of more than 30%, superior electrical conductivities of over 1000 S/cm at intermediate temperatures (600–800 °C), a moderate average thermal coefficient of $12.6–13.5 \times 10^{-6}$ between 100 and 800 °C and excellent bending strength of around 100 MPa.

Keywords: Powders-chemical preparation; Porosity; Electrical conductivity; Thermal expansion; Strength; Fuel cells

1. Introduction

Solid oxide fuel cells (SOFCs) are energy conversion devices with high efficiency and various environmental advantages. Conventional SOFCs based on yttria-stabilized zirconia (YSZ) electrolytes have to operate between 950 and 1000 °C, because of the lower ionic conductivity of the YSZ solid electrolyte at lower operating temperatures. However, these high operating temperatures often lead to serious problems such as chemical reactions and thermal expansion mismatch between the SOFC components.[1] Current research efforts are aimed at reducing the operating temperatures to 600–800 °C or less. Sm^{3+} doped CeO_2 (SDC) has been regarded as the most promising electrolyte for intermediate temperature SOFCs (IT-SOFCs) because of its excellent ionic conductivity compared to YSZ.[2,3] The most suitable anode for SDC electrolyte-based SOFCs is generally thought to be Ni–samaria-doped ceria (Ni–SDC cermets).[1,4]

Over the past few years, Ni–YSZ cermet anode has been successfully applied to YSZ electrolyte-based single cells.[5,6] Comparatively, the Ni–SDC cermet anode has various advantages derived from the extraordinary properties of the SDC compositions. SDC is an ion-and-electron mixed conductor in hydrogen, which can increase the length of triple phase boundary (TPB) within the anode.[7] Moreover, SDC also exhibits oxidation-catalytic properties and high anodic activities due to its rapid electrochemical oxidation of hydrocarbon gas.[8] Therefore, Ni–SDC cermets can be considered as a promising candidate for IT-SOFC anode. However, most of the previous works related to Ni–SDC anodes were concentrated on their electrical conducting and electrochemical properties, regarding the Ni–SDC cermet as an excellent hydrogen oxidation catalyst as well as a effective ion-and-electron mixed conductor at intermediate temperatures.[9–11] For their application in SOFCs, a prominent design for the cell stacks is the anode-supported one, which sustains mechanical stress in the single cell and allows the thickness of the electrolyte to be reduced.[12] In view of the long-term stability required for SOFCs during their operation and movement, it is necessary to investigate the thermal expansion and mechanical properties of Ni–samaria-doped ceria cermets.

---

[*] Corresponding author. Tel.: +82 63 270 2380; fax: +82 63 270 2386.
[**] Corresponding author. Tel.: +86 27 87863277; fax: +86 27 87864580.
E-mail addresses: kimbh@chonbuk.ac.kr (B.H. Kim), xuqing@mail.whut.edu.cn (Q. Xu).

0955-2219/$ – see front matter © 2008 Elsevier Ltd. All rights reserved.
doi:10.1016/j.jeurceramsoc.2008.05.009

Considering that the traditionally mechanical mixing process, in which the separately prepared NiO and SDC powders are simply mixed together by ball milling to act as anodic initial powders, cannot result in the reliable uniform distribution of Ni particles in the Ni–SDC matrix,[4,10] a urea-combustion technique was employed in our study to fabricate the NiO–SDC composite powders in one step. The urea-combustion technique had been successfully employed to produce the initial powders for SOFC materials, such as SDC electrolytes and Ni–YSZ anodes.[13,14] High temperatures could reach in a short reaction time by the self-generated heat of reaction, yielding nanopowders or loose agglomerate of nanocrystallites. Given the above considerations, in this work, NiO–SDC composite powders were produced by the urea-combustion technique and the structure, electrical conducting, thermal expansion and mechanical properties of the Ni–SDC cermets were investigated with respect to the volume contents of Ni (Ni vol.%).

2. Experimental procedure

Reagent grade $Ni(NO_3)_2{\cdot}6H_2O$, $Ce(NO_3)_3{\cdot}6H_2O$, $Sm(NO_3)_3{\cdot}6H_2O$ and $CO(NH_2)_2$ (urea) were used as starting materials and dissolved into deionized water to form a solution. The nitrates were weighted in suitable proportion for the Ni vol.% in the Ni–SDC cermets to be in the range of 30–70 vol.%. Hereafter, the Ni–SDC composites were designated as x%Ni–SDC ($x = 30$–70). The amount of urea for the formation of the NiO–SDC composite powders can be calculated according to the following equations:

$$3Ni(NO_3)_2{\cdot}6H_2O + 5CO(NH_2)_2 = 3NiO + 8N_2 + 5CO_2 + 28H_2O \quad (1)$$

$$8Ce(NO_3)_3{\cdot}6H_2O + 2Sm(NO_3)_3{\cdot}6H_2O + 30CO(NH_2)_2 = 10Ce_{0.8}Sm_{0.2}O_{1.9} + 45N_2 + 30CO_2 + 120H_2O \quad (2)$$

In this case, 1 mol NiO and 1 mol SDC stoichiometrically require 5/3 and 3 mol urea, respectively. If we designate the total metal cation content in each composition to be 0.05 mol, the amount of urea can be subsequently determined using the density of Ni (8.90 g/cm^3) and SDC (7.15 g/cm^3),[15,16] as presented in Table 1. It can be noticed that the amount of urea is around 0.1 mol, which is almost twice the total metal cation content in each composition. Therefore, the mole ratio of urea to the total metal cation content was selected as 2.0 in this study. Once it was prepared, the solution was stirred for 1 h and heated on a hot plate until auto-ignition and self-sustaining combustion occurred. The ash was subsequently ground for 48 h in ethanol medium using a ball milling process with zirconia balls. After the slurry was dried, the as-synthesized powders were uniaxially pressed into disks (10 mm in diameter and 1 mm in thickness) and rectangular bars (40 mm × 4 mm × 4 mm) under a pressure of 100 MPa, followed by sintering at 1200–1300 °C for 4 h in air and reducing at 800 °C for 2 h in a $60\%N_2 + 40\%H_2$ atmosphere.

Table 1
The amount of urea for the formation of NiO–SDC composite powders

Compositions	NiO (mol)	SDC (mol)	Urea (mol)
30%Ni–SDC	0.0305	0.0195	0.1093
40%Ni–SDC	0.0355	0.0145	0.1029
50%Ni–SDC	0.0396	0.0104	0.0972
60%Ni–SDC	0.0423	0.0077	0.0936
70%Ni–SDC	0.0448	0.0052	0.0903

The phase identification of the as-synthesized powders and reduced specimens was examined by a Rigaku D/MAX-111A X-ray diffractometer using Cu Kα radiation. The morphology of the as-synthesized powders was observed using a Jeol JSM-6400 scanning electron microscope (SEM) and a Hitachi S-4700 field emission scanning electron microscope (FESEM) at different magnifications. The microstructure of the sintered and reduced specimens was investigated by means of SEM combined with back scattering electron (BSE) microscopy. The density and open porosity of the Ni–SDC cermets were measured by the Archimedes method using disk-type cermets, in accordance with China standard no. GB/T 1966-1996.

The rectangular cermets were polished to ensure their surface flatness and painted with platinum paste for the purpose of measuring the electrical conductivity. The electrical conductivity of the specimens was measured by a dc four-probe method at 350–800 °C in a $60\%N_2 + 40\%H_2$ atmosphere. The thermal expansion measurement was conducted using rectangular cermets upon heating in an Ar atmosphere at a heating rate of 5 °C min^{-1} between 100 and 800 °C by a Netzsch DIL 402C dilatometer with alumina as a calibration standard. The three-point bending strength of the Ni–SDC cermets (30 mm × 2.5 mm × 2.5 mm) was evaluated using a universal testing machine (5802 Engineer Dr., United Calibration Corp.) with a fixture of 25 mm span and crosshead speed of 1 mm min^{-1} at room temperature. The highest value and the lowest value were excluded from the calculations of the average value and the standard deviation of the bending strength.

3. Result and discussion

Fig. 1 shows the XRD patterns of the as-synthesized powders with various Ni vol.%. Both NiO and SDC phases were certified for the powders and no other phase could be found within the sensitivity of XRD. Fig. 2 shows the typical morphology of the as-synthesized powders, consisting of homogenous and weakly agglomerated particles around 40–150 nm.

Fig. 3 shows the XRD patterns of the Ni–SDC cermets prepared by sintering at 1300 °C for 4 h in air and reduction at 800 °C for 2 h in a $60\%N_2 + 40\%H_2$ atmosphere. As can be seen, the peaks presented in the XRD patterns are assignable to the two constituents and the relative intensity of the peaks corresponding to the Ni phase increases with increasing Ni vol.%. Namely, no remarkable reaction product between the Ni and SDC can be detected within the sensitivity of XRD after the sintering and reducing process.

Fig. 4 shows the open porosity of the Ni–SDC cermets prepared by sintering at 1200–1300 °C for 4 h in air and reduction at 800 °C for 2 h in a $60\%N_2 + 40\%H_2$ atmosphere as a function of

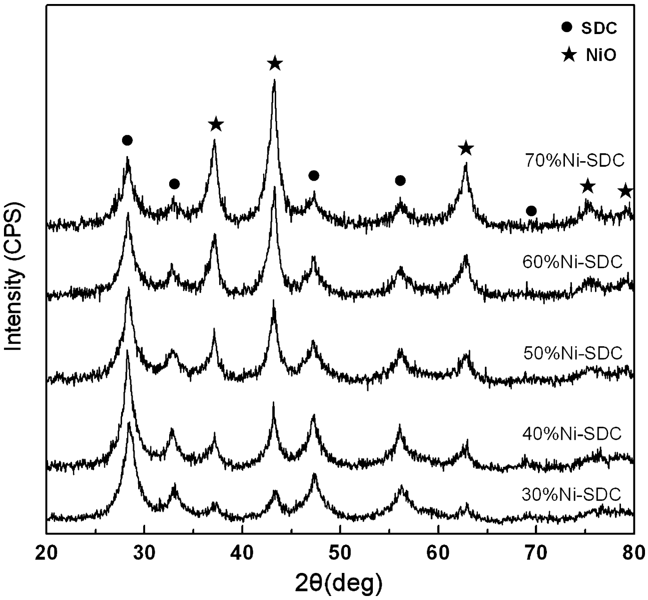

Fig. 1. XRD patterns of the as-synthesized powders with various Ni vol.%.

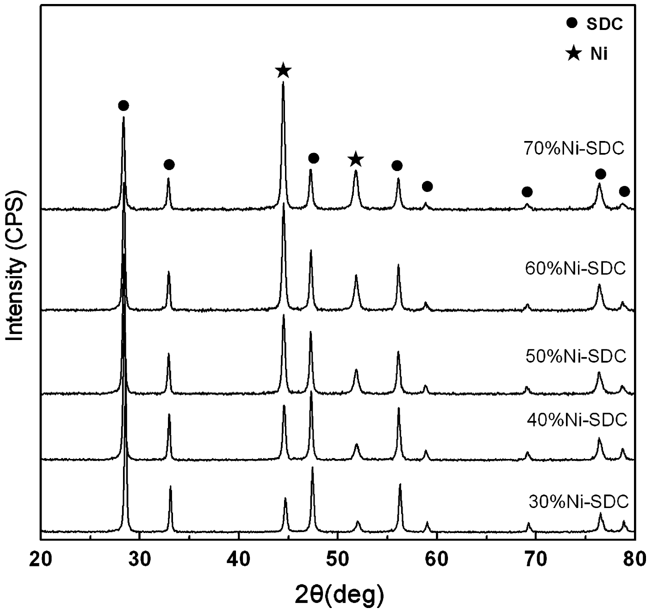

Fig. 3. XRD patterns of the Ni–SDC cermets with various Ni vol.%.

the Ni vol.%. The open porosity of each composition decreases with elevated sintering temperatures as expected. In the case of the samples sintered at the same temperatures, the open porosity of the specimens displays an identical variation with the Ni vol.%, increasing with Ni vol.% up to a maximum value and then decreases. As is well known, the pores in the Ni–SDC cermets are mainly formed by the reduction of NiO. Therefore, it is not surprising that the open porosity of the cermets increases with increasing Ni vol.%. However, for the 70%Ni–SDC specimen, the open porosity decreased, which may be due to the microstructural changes. Regarding an open porosity of 30% as a criterion for gas transport inside the anode,[11,17] the cermets prepared by sintering at 1300 °C should be excluded, due to their lower values of the open porosity. Besides, during the processing of an anode-supported single cell, the anode material is always co-sintered with the electrolyte material. In our previous research, the SDC materials were able to be sintered to a relative density of 95.8% at a sintering temperature of 1250 °C. However, when the samples were sintered at 1200 °C, the relative density of the SDC ceramics was around 90%, which is not suitable for an SOFC electrolyte, because of the resulting gas leak. Hence, to facilitate the co-sintering of the Ni–SDC anode and SDC electrolyte, the cermets prepared by sintering at 1250 °C for 4 h in air and reduction at 800 °C for 2 h in a 60%N_2 + 40%H_2 atmosphere (abbreviated as 1250Ni–SDC) were selected for investigation in our following research.

Fig. 5 shows the BSE images of the NiO–SDC ceramics sintered at 1250 °C with various Ni vol.%. The SEM images of the corresponding specimens are presented in the insets. A dense microstructure consisting of homogeneously dispersed NiO and SDC phases can be observed, where the black domains corresponding to the NiO phases gradually expand with increasing

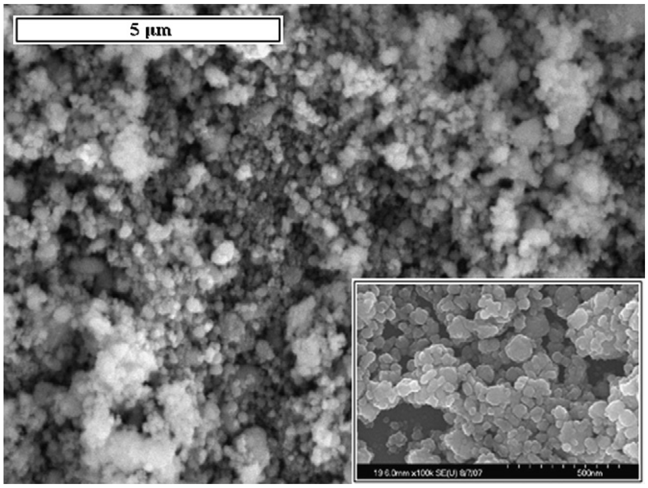

Fig. 2. SEM and FESEM micrographs of the as-synthesized powders containing 50 vol.% Ni.

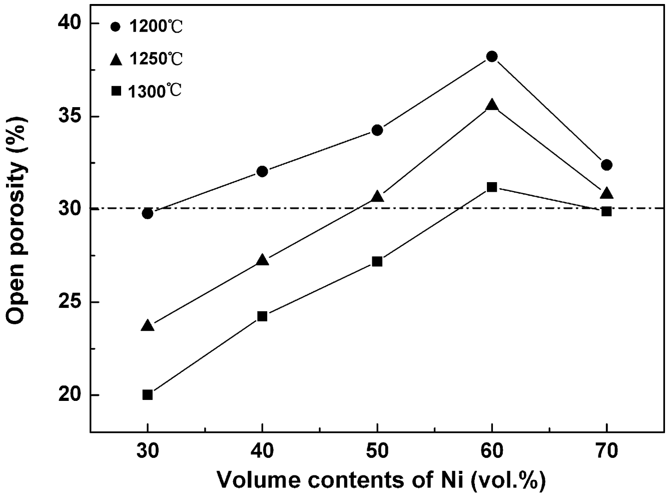

Fig. 4. Open porosity of the Ni–SDC cermets prepared by sintering at 1200–1300 °C for 4 h in air and reduction at 800 °C for 2 h in 60%N_2 + 40%H_2 atmosphere as a function of Ni vol.%.

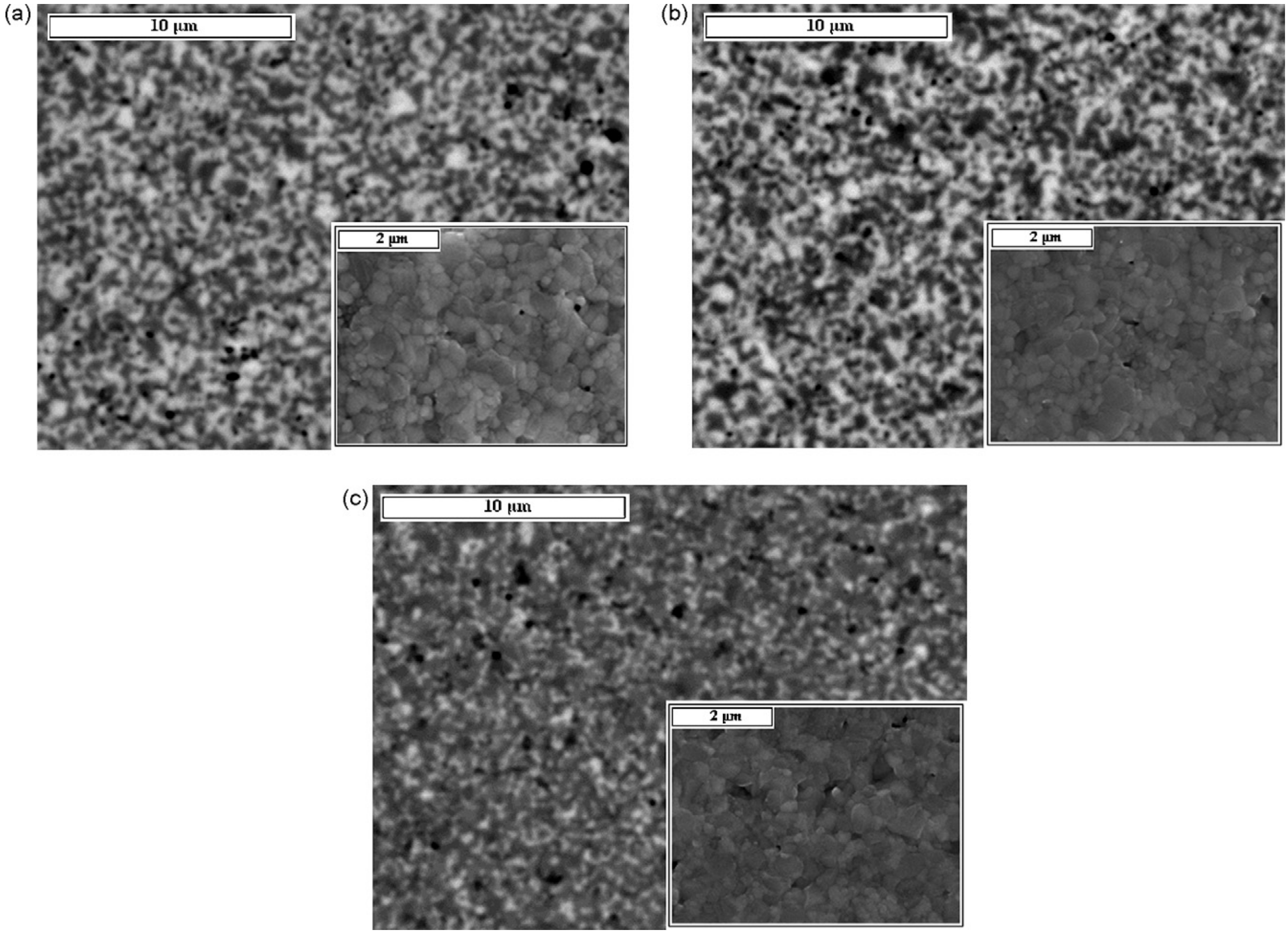

Fig. 5. BSE and SEM images of the NiO–SDC ceramics sintered at 1250 °C with (a) 30 vol.% Ni, (b) 50 vol.% Ni, (c) 70 vol.% Ni.

Ni vol.%. One can also see that both the dark domains and white domains are continuous, indicating the presence of well-connected grains of NiO–NiO and SDC–SDC in the cermets.

Fig. 6 shows the SEM micrographs of 1250Ni–SDC cermets with various Ni vol.%. When the Ni vol.% is from 30% to 60%, the good connection among the grains as well as the uniform distribution of the submicron-sized grains and pores can be seen in the cermets. These characteristics of the microstructure would contribute to optimize the length of the Ni–SDC–gas triple phase boundary (TPB) and, thus, improve the anodic performance.[7] However, the microstructure of the 70%Ni–SDC cermet is different from that of the other compositions, displaying a lot of clusters together with weakly connected small grains. As is generally recognized, SDC components play an important role in suppressing the sintering of Ni during the preparation of the Ni–SDC cermets.[18] Hence, it can be imagined that if the SDC content is as lower as 30 vol.%, as in the case of the 70%Ni–SDC cermet, the function of the SDC as a secondary phase would become relatively weak, resulting in the appearance of aggregated Ni grains and weakly contact among the SDC grains. This is assumed to be responsible for the reduced open porosity in Fig. 4. The performances of SOFC anodes are governed by the electronic conductivity of the electrocatalysts such as nickel, the overpotentials associated with the charge-transfer at the TPB, the ionic conductivity of the electrolytes and the rate of gas transport through the porous electrodes. Furthermore, the rate of electronic and ionic transport is a function of microstructural variables such as the grain size and continuity of the grains.[19] As shown in Fig. 6(d), the cermet consisted of many large grains due to the Ni aggregation and weakly connected SDC grains, which may induce the deterioration of the anodic performance.

Fig. 7 shows the electrical conductivity of the 1250Ni–SDC cermets as a function of measuring temperature. At the same measuring temperature, the electrical conductivities increase with increasing Ni vol.% as expected. Also, a monotonous decrease in the electrical conductivities can be observed with increasing measuring temperature in the range of 350–800 °C. Such conducting behavior is similar to that of a metallic electronic conductor and to the previously reported results,[4,11] indicating that the Ni component dominates the electrical conducting properties of the Ni–SDC matrix. Moreover, it was noted that all of the compositions provide electrical conductivities over 600 S/cm at intermediate temperatures (600–800 °C), exceeding the electrical conductivity requirement for the anode material of SOFCs.[20] This result is in agreement with the continuous NiO grains and Ni grains observed in Figs. 5 and 6, respectively, even when the Ni vol.% is as low as 30%.

It can also be noticed that the electrical conductivity at 600–800 °C in this study is superior to that of the Ni–SDC cermets with the same Ni vol.% prepared by other processes, such

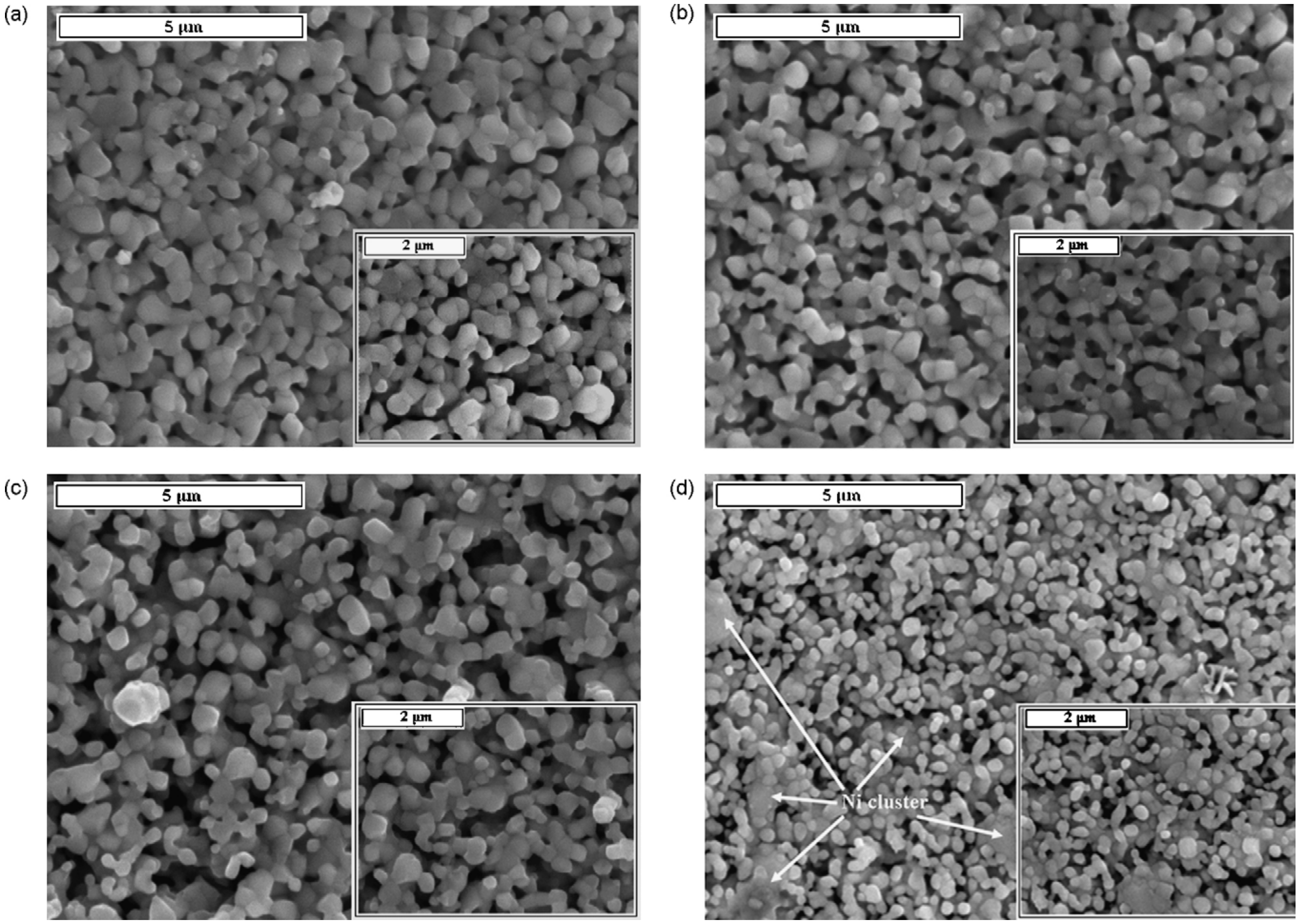

Fig. 6. SEM micrographs of 1250Ni–SDC cermets with (a) 30%Ni–SDC, (b) 50%Ni–SDC, (c) 60%Ni–SDC, (d) 70%Ni–SDC.

as mechanical mixing, co-precipitation and gel-casting,[4,11,21] whereas comparable with Ni–YSZ cermets.[22] According to the percolation theory, in a binary composite consisting of conductive and insulating phases, coarse particles are expected to be surrounded by finer insulating particles and inhibit the contact among conductive particles.[23] As regards the NiO–SDC composite powders, SDC can be considered as an insulating phase, because of its low ionic conductivity (~0.08 S/cm at 800 °C),[24] while NiO was known as conductive phase due to its superior electronic conductivity after being reduced to Ni. In the case where the coarse NiO particles and fine SDC particles were prepared by other processes, the coarse NiO particles appeared to be covered by fine SDC particles. The isolated Ni grains after reduction would not contribute to the electrical conductivity of the Ni–SDC cermets. However, if fine NiO particles can be dispersed well with SDC particles, as in the case of our research, then well-connected Ni grains can be obtained after reduction. Based on the above analyses, we can conclude that fine and uniformly distributed NiO–SDC composite powders can be fabricated through the urea-combustion technique. This is presumably responsible for the excellent electrical conductivity of the Ni–SDC cermets in this work.

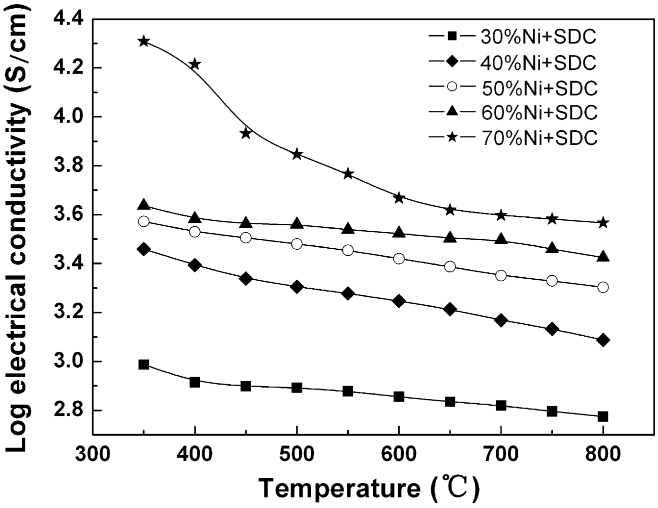

Fig. 7. Electrical conductivity of the 1250Ni–SDC cermets as a function of measuring temperature.

Fig. 8 shows the linear thermal expansion curves (LTECs) of the 1250Ni–SDC cermets. For each specimen, the LTEC seems to be a straight line except for the anomalous variation between 350 and 400 °C. To characterize this anomaly in a more accurate way, the differential coefficients of the corresponding LTECs were resolved, as shown in the inset of Fig. 8. The peaks marked as T^* appear in the temperature range of 360–400 °C, as expected. This behavior is also typical for Ni–YSZ cermets

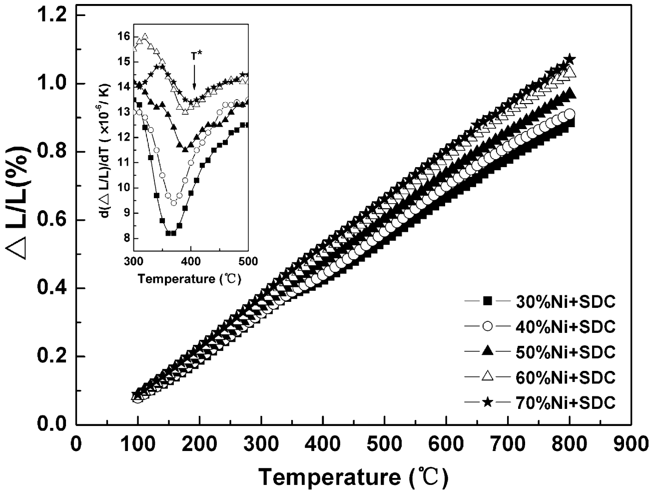

Fig. 8. Linear thermal expansion curves of the 1250Ni–SDC cermets with various Ni vol.%.

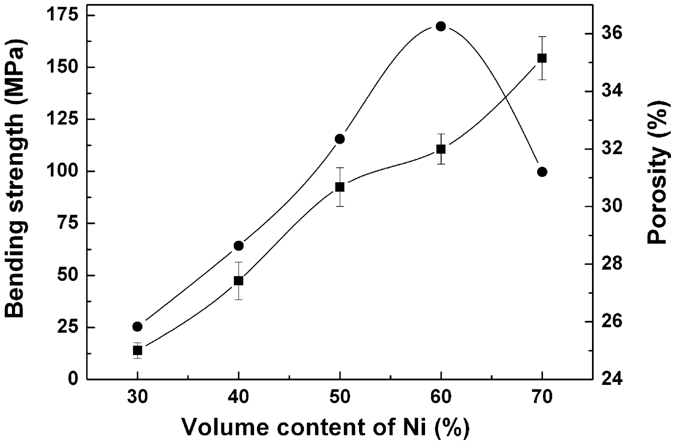

Fig. 9. Bending strength and porosity of the 1250Ni–SDC cermets as a function of Ni vol.%.

and can be explained by the large anomaly of the Young's modulus of Ni near T_c (Curie point), due to the ferromagnetic-to-paramagnetic phase transition.[16,25] One can also notice that there is tendency for T^* to increase with increasing Ni vol.%. This phenomenon can be qualitatively interpreted by the evolution of Ni grains in the Ni–SDC cermets. As shown in Fig. 6, it is unfeasible to distinguish the Ni grains from the SDC grains in the 30–60%Ni–SDC cermets, owing to their similar grain size. However, as for the 70%Ni–SDC specimen, aggregated Ni grains with a large size can be clearly observed. Compared with the large Ni grains, the small Ni grains are under higher pressure due to their intense surface extension, which would promote the phase transition of Ni at a lower temperature.[26] The shift of T^* toward higher temperatures may reflect the growth of the Ni grains with increasing Ni vol.% in the cermets.

The average thermal expansion coefficient (TEC) values were calculated in the whole temperature range of 100–800 °C, the lower temperature range of 100–T^* and the high temperature range of T^*–800 °C. The calculated results are listed in Table 2. For each specimen, the average TEC in the high temperature range is always slightly lower than that in the lower temperature range. This result implies that the LTEC of the 1250Ni–SDC cermets can be approximated by two straight lines, with a decrease in the slope occurring at T^*. In the same temperature range, the average TECs of the cermets seem to be dominated by the Ni content, increasing monotonously with increasing Ni vol.%, which can be explained by the large TEC of Ni metal (16.9×10^{-6}/K) compared with that of SDC (12.8×10^{-6}/K).[16,27] Moreover, in the overall temperature range, the TEC value difference between the 1250Ni–SDC anode and SDC electrolyte is within the limits acceptable to thermodynamic compatibility (15–20%),[27] with the composition of 30–60%Ni–SDC showing the most promising performance in terms of the thermal expansion matching.

The bending strength and porosity of the 1250Ni–SDC cermets is plotted as a function of Ni vol.% in Fig. 9. The cermets with Ni vol.% of 50–70% offer excellent bending strengths of 93–154 MPa, satisfying the requirement of the mechanical properties for an anode-supported material. Moreover, the bending strength was found to increase with the increasing Ni vol.%. As is well known, the relationship between strength (σ) and porosity (p), can be described by:

$$\sigma = \sigma_0 \exp(-bp), \tag{3}$$

where σ_0 is the strength of the non-porous structure and b is a pre-exponential coefficient related to the pore structure.[12] If non-porous Ni–SDC cermets could be obtained, it is reasonably to suggest that the value of σ_0 would increase with increasing Ni vol.%, thus affecting the value of σ in a positive way. This deduction can be explained by the mechanism of strengthening and toughening. Generally speaking, the bending strength and fracture toughness of ceramics are much lower than those of metals. When pressing the cermets under an external force, the metallic grains undergo plastic deformation by absorbing plastic energy. During the spreading of the cracks, the plastic deformation of the metallic grains could induce the passivation on the tip of the cracks and the decrease of the stress intensity factor. As

Table 2
Average TEC values in various temperature ranges for 1250Ni–SDC cermets

Compositions	Average TEC ($\times 10^{-6}$/K)		
	Whole temperature range (°C)	Low temperature range (°C)	High temperature range (°C)
30%Ni–SDC	11.1 (100–800)	11.9 (100–360)	10.6 (360–800)
40%Ni–SDC	11.9 (100–800)	12.2 (100–370)	11.7 (370–800)
50%Ni–SDC	12.6 (100–800)	13.1 (100–390)	12.3 (390–800)
60%Ni–SDC	13.5 (100–800)	14.0 (100–390)	13.2 (390–800)
70%Ni–SDC	14.0 (100–800)	14.5 (100–400)	13.7 (400–800)

the interface between metal and ceramic starts to split, the cracks would turn around and branch off by means of absorbing fracture energy, which prevents the further extension of the crack.[28] On the other, the porosity of the cermets in Fig. 9 generally increases with increasing Ni vol.% except for the 70%Ni–SDC sample, resulting in a negative effect on the value of σ. Based on the above analyses, we can conclude that the bending strength of the Ni–SDC cermets is mainly dependent on two competitive factors: Ni vol.% and porosity, with the effect of Ni vol.% predominating the variation of the bending strength.

4. Conclusions

The urea-combustion technique was shown to be an advantageous route to produce NiO–SDC composite powders. The structure, electrical conducting, thermal expansion and mechanical properties of the resulting Ni–SDC cermets were investigated with respect to the Ni vol.%. No chemical reaction product between the two constituent phases was detected for the cermets sintered at 1200–1300 °C for 4 h in air and reduced at 800 °C for 2 h in a $60\%N_2 + 40\%H_2$ atmosphere. The cermets with 30–60Ni vol.% showed a porous microstructure composed of uniformly distributed and well-connected constituent grains. However, further increasing the Ni vol.% induced the generation of aggregated grains derived from the Ni sintering. For each specimen, the electrical conducting and thermal expansion properties seem to be competent for anode materials. Nevertheless, the open porosity and bending strength are sensitive to the Ni vol.%. Adequately controlling the composition in the cermets allows them to benefit from the superior electrical conductivity, bending strength and open porosity of Ni, together with low TEC of the SDC. The trade-off among the structure, electrical conducting, thermal expansion and mechanical properties results in the optimum composition being obtained for the cermets containing 50–60 vol.% Ni.

Acknowledgements

This work was financially supported by the International Collaboration Program of Jeonbuk Province and Korea Research Foundation Grant funded by the Korean Government (MOEHRD, KRF-2007-211-D00053). It is grateful to the Ministry of Knowledge Economy (MKE) through the Specialized Graduate School program. The authors are also thankful to the Natural Science Foundation of China (Grant No. 50572079) for supporting this research.

References

1. Molenda, J., Swierczek, K. and Zajac, W., Functional materials for the IT-SOFC. *J. Power Source*, 2007, **173**, 657–670.
2. Kilner, J. A., Fast anion transport in solids. *Solid State Ionics*, 1983, **8**, 201–207.
3. Anderson, R. G. and Nowick, A. S., Ionic conductivity of CeO_2 with trivalent dopants of different ionic radii. *Solid State Ionics*, 1981, **5**, 547–550.
4. Fang, X. H., Zhu, G. Y., Xia, C. R., Liu, X. Q. and Meng, G. Y., Synthesis and properties of Ni-SDC cermets for IT-SOFC anode by co-precipitation. *Solid State Ionics*, 2004, **168**, 31–36.
5. Du, Y. H. and Sammes, N. M., Fabrication and properties of anode-supported tubular solid oxide fuel cells. *J. Power Source*, 2004, **136**, 66–71.
6. Zhang, L., Jiang, S. P., Wang, W. and Zhang, Y. J., NiO/YSZ, anode-supported, thin-electrolyte, solid oxide fuel cells fabricated by gel casting. *J. Power Source*, 2007, **170**, 55–60.
7. Sun, C. W. and Stimming, U., Recent anode advances in solid oxide fuel cells. *J. Power Source*, 2007, **171**, 247–260.
8. Zhao, S. and Gorte, R. J., A comparison of ceria and Sm-doped ceria for hydrocarbon oxidation reactions. *Appl. Catal. A: Gen.*, 2004, **277**. pp. 129–126.
9. Maric, R., Ohara, S., Fukui, T., Inagaki, T. and Fujita, J. I., High-performance Ni-SDC cermet anode for solid oxide fuel cells at medium operating temperature. *J. Electrochem. Soc.*, 1998, **1**(5), 201–203.
10. Yin, Y. H., Li, S. Y., Xia, C. R. and Meng, G. Y., Electrochemical performance of gel-cast NiO-SDC composite anodes in low-temperature SOFCs. *Electrochim. Acta*, 2006, **51**, 2594–2598.
11. Yin, Y. H., Zhu, W. Y., Xia, C. R. and Meng, G. Y., Gel-cast NiO-SDC composites as anodes for solid oxide fuel cells. *J. Power Source*, 2004, **132**, 36–41.
12. Yu, J. H., Park, G. W., Lee, S. W. and Woo, S. K., Microstructural effects on the electrical and mechanical properties of Ni-YSZ cermet for SOFC anode. *J. Power Source*, 2007, **163**, 926–932.
13. Chinarro, E., Jurado, J. R. and Colomer, M. T., Synthesis of ceria-based electrolyte nanometric powders by urea-combustion technique. *J. Eur. Ceram. Soc.*, 2007, **27**, 3619–3623.
14. Ringuede, A., Labrincha, J. A. and Frade, J. R., A combustion synthesis method to obtain alternative cermet materials for SOFC anodes. *Solid State Ionics*, 2001, 549–557.
15. Li, H. B., Xia, C. R., Zhu, M. H., Zhou, Z. X. and Meng, G. Y., Reactive $Ce_{0.8}Sm_{0.2}O_{1.9}$ powder synthesized by carbonate coprecipitation: sintering and electrical characteristic. *Acta Mater.*, 2006, **54**, 721–727.
16. Mori, M., Yamamoto, T., Itoh, H., Inaba, H. and Tagawa, H., Thermal expansion of nickel-zirconia anodes in solid oxide fuel cells during fabrication and operation. *J. Electrochem. Soc.*, 1998, **145**, 1374–1381.
17. Dees, D. W., Claar, T. D., Easler, T. E., Fee, D. C. and Mrazek, F. C., Conductivity of porous Ni/ZrO_2-Y_2O_3 cermets. *J. Electrochem. Soc.*, 1987, 2141–2146.
18. Okawa, Y. and Hirata, Y., Sinterability, microstructure and electrical properties of Ni/Sm-doped ceria cermet processed with nanometer-sized particles. *J. Eur. Ceram. Soc.*, 2005, **25**, 473–480.
19. Lee, J. H., Heo, J. W., Lee, D. S., Kim, J., Kim, G. H., Lee, H. W., Song, H. S. and Moon, J. H., The impact of anode microstructure on the power generating characteristics of SOFC. *Solid State Ionics*, 2003, **158**, 225–232.
20. Minh, N. Q. and Takahashi, T., *Science and technology of ceramics fuel cells*. Elsevier, Califorlia, 1995, pp. 147–149.
21. Cheng, J. G., Deng, L. P., Zhang, B. R., Shi, P. and Meng, G. Y., Properties and microstructure of NiO/SDC materials for SOFC anode applitions. *Rare metals*, 2007, **26**, 110–117.
22. Anselmi, T. U., Chiodelli, G., Arimondi, M., Maglia, F., Spinolo, G. and Munir, Z. A., Electrical properties of Ni/YSZ cermets obtained through combustion synthesis. *Solid State Ionics*, 1998, **110**, 35–43.
23. Mclachlan, D. S., Blaszkiewicz, M. and Newnhan, R. E., Electrical resistivity of composites. *J. Am. Ceram. Soc.*, 1990, **73**, 2187–2203.
24. Peng, R. R., Xia, C. R., Fu, Q. X., Meng, G. Y. and Peng, D. K., Sintering and electrical properties of $(CeO_2)_{0.8}(Sm_2O_3)_{0.1}$ powders prepared by glycine-nitrate process. *Mater. Lett.*, 2002, **56**, 1043–1047.
25. Soeffge, F., Steichele, E. and Stierstadt, K., Thermal expansion anomaly of nickel near the Curie point. *Phys. Status Solidi A*, 1977, **42**, 621–627.
26. Aaronson and Hubert, I., *Lectures on the theory of phase transformations*. Minerals, Metals, & Materials Society, New York, 1982, pp. 65–75.
27. Xu, Q., Huang, D. P., Zhang, F., Chen, W., Chen, M. and Liu, H. X., Structure, electrical conducting and thermal expansion properties of $La_{0.6}Sr_{0.4}Co_{0.8}Fe_{0.2}O_{3-\delta}$-$Ce_{0.8}Sm_{0.2}O_{2-\delta}$ composite cathodes. *J. Alloy Compd.*, 2008, **454**, 460–465.
28. Huang, P. Y., *Powder metallurgical theory*. Metallurgical Industrial Press, Beijing, 1997, pp. 265–331.